EasyChair Preprint

№ 10350

Ground Granulated Blast Furnace Slag Blended with Silica Fume and Activated with Hydrated Lime: a Short Communication

Jayashree Sengupta and Nirjhar Dhang

June 7, 2023

Ground Granulated Blast Furnace Slag blended with Silica Fume and Activated with Hydrated Lime: A Short Communication

Jayashree Sengupta[1], Nirjhar Dhang[2]

[1]Research Scholar, Dept. of Civil Engineering, Indian Institute of Technology, Kharagpur, West Bengal 721302, India (corresponding author). ORCID: https://orcid.org/0000-0002-6892-3480.

Email: jaish.sengupta@iitkgp.ac.in

[2]Professor, Dept. of Civil Engineering, Indian Institute of Technology, Kharagpur, West Bengal 721302, India.

Email: nirjhar@civil.iitkgp.ac.in

Abstract

The goal of this study is to see if industrial grade hydrated lime can be used as an alkali activator in a one-part system. Calcium addition has long been shown to be beneficial to alkali-activated concrete in studies. The results of this study, however, revealed that using hydrated lime as the sole activator did not significantly increase the strength. This was because calcium-based activators did not improve system pH as much as sodium-based counterparts did. Crystal formations of ettringite and thaumasite were also observed in the microstructure. Furthermore, the pozzolanic reactions overtook the polymerization reaction, resulting in medium strength.

Keywords

Lime-activated slag mortar, ground-granulated blast furnace slag, alkali activation, microstructure

1. Introduction

There is a pressing need for raw building materials that are both environmentally and technically sound alternatives to standard cementitious concrete. The manufacture of concrete and other

commonly used building materials consumes a lot of energy and emits a lot of CO_2. Nonetheless, concrete will remain the primary building material for many years to come. As a result, greener concrete becomes more necessary. Alkali-activated concretes fundamentally recycle industrial waste into aluminosilicate precursors, which develop binding properties when activated by alkalis. In the process, cement is completely replaced. In comparison to OPC, it has reportedly improved mechanical properties. However, its wide-scale application is limited due to the handling of toxic and harmful alkali solutions. For the in-situ castings, alkali-activated concrete would also need skilled labour. Hence, alkali-activated mixes are divided into two-part mixes and one-part mixes. The latter is a dry mixture of the solid activators, additives, and precursors that have already been dry-blended to create a single binder. This is equivalent to the common practice of concreting due to the powdered form and "just-add-water" methodology. Thus, the one-part geopolymer mixes contribute to the greening of concrete by reducing the amount of cement while replacing it entirely or mostly with an aluminosilicate precursor material, managing waste by recycling industrial by-products like slag, fly ash, etc. as precursors, and enabling user-friendly in-situ casting without the use of caustic solutions.

In the two-part geopolymers, the precursor materials were activated by highly caustic alkaline solutions. By altering the mix's pH, these activators initiated the dissolution process. The activators could be basic or acidic. The most common activators come from the alkali family (Na^+, K^+) and alkali earth (Ca^{+2}, Mg^{+2}). The acidic family includes H_3PO_4 [1, 2, 3, 4, 5, 6] and citric acid [7] although the hydrates may not be stable products [8]. Even for one-part geopolymer, the alkali particles dissolve, followed by the release of hydroxyl ions, which raises the pH of the system, which then engages in network formation with the release of silica and alumina. In due course of time, the pH is lowered with the intake of OH^- ions. Thus, the presence of OH^- ions catalyse ion exchange during the hydrolysis-deprotonating of the aluminosilicate precursor's susceptible Si-O-Si bonds, which can also be initiated and enhanced by mechanochemical processing [9]. Because of their weaker nature, Si-O-Si bonds tended to dissolve faster at pH >11, whereas Al-O bonds dissolved faster at pH >6. The addition of calcium, on the other hand, resulted in a stable 3D framework at pH <12 [10]. According

to [11], the presence of calcium-rich phases had a beneficial effect on mechanical strength because the formation of two distinct phases of CSH and the polymeric gel, which bridged and densified the microstructure, increases the mechanical strength. The hydroxyl groups and the divalent calcium ion reacted to form a precipitate, raising the pH and delivering sites for the silicates' polymerization and nucleation [12]. Thus, the availability of the calcium ions and the pH of the mixture were key factors in the continuous formation of the binding gels of CSH, CASH, and NCASH. The amount of calcium ions present should be sufficient to promote the reaction between the tetrahedrons made of silicate and aluminate [13]. Aside from highly reactive alkali solutions, the addition of calcium ions to precursors such as clay from the brick industry proved to be a favourable alternative for improving mechanical properties [14]. However, dissolution has been reported [15] to be delayed, as has oligomer formation, brought on by Lewis acidity competition between the alkali cations Ca^{+2} and Na^{+}. As a result, the sole effect of using hydrated lime as a solid activator is an intriguing area of study.

Hydraulic lime was already an ideal building material before the invention of cement. The strength and durability properties of lime-pozzolana mixes were reported in the literature [16, 17], and the ancient Greeks and Romans valued the mixing of lime mortars with reactive aluminosilicates [18, 19]. Lime could be used as an alkali activator, in addition to being a building material. The precipitation of phillipsite and Al-tobermorite crystals as a result of the reaction with seawater, as well as ionic exchanges with pozzolanic alkaline aggregates and seawater, was reported to have strengthened the roman concrete over time. Thus, set the niche of geopolymer, as coined by Davidovits [20]. The pozzolanic reactivity and curing conditions played a significant role in dominating the carbonation reaction, in the hydration process of typical lime-pozzolanic blends [21]. To ensure adequate strength during the hydration reactions, lime-pozzolana mortars needed moist regimes. In dry regimes, the hydration reactions slowed down or even stopped by the full carbonation of the lime. Therefore, a significant issue that needed to be addressed was the degree of carbonation in high calcium mixes. In [22], the authors investigated the effects of adding nano-silica and nano-

alumina to lime-pozzolana blends. Their findings might provide a potential solution to the aforementioned carbonation implication. The nano-silica reduced the porosity and carbonation values while increasing the compressive strength of the mix. Also, a densified microstructure was reported [23]. Thus, the addition of silica might be advantageous when activated by hydrated lime.

With the help of these findings, the notion automatically switches to the reactive aluminosilicate set of binders and the resulting modifications in the mix's properties. A detailed investigation of the characteristics connected with specific by-products was carried out [24]. The paper can be used to comprehend the advantages of each precursor as well as the ambiguities that remain unresolved. Alkali-activated binders were described as the "epicenter" of cement technology in a thorough overview by [25] levying their potential and range. The industrial by-products showing pozzolanic properties [26, 27, 28, 29, 24] were reported to be suitable aluminosilicate precursors for geopolymers [30] and had been the focus of research for the last few decades. Luukkonen et al. [31] provided a thorough analysis of the merits and demerits of one-part alkali-activated binders as a workable engineering component for environment-friendly concrete production. Such concrete was observed to have less strength because of increased crystalline zeolitic formation. With the help of silica fume and red mud, [32] good strength was reported. The microstructure was typically weakened by crystallinity [33], but in alkali-activated mixes, the amorphous gel strengthened the ITZ and contributed to the improvement in strength. By regulating the water content in one-part geopolymers, crystalline microstructure formation could be prevented [34]. Due to the hydration of the CaO content in GGBFS, the additional SiO_2 of rice husk ash resulted in enough strength by forming additional CSH gel [35]. The matrix was denser by the simultaneous formation of the two binding gels. The undissolved phase of excess silica was visible during the first few days of curing, but it eventually vanished [32]. In the presence of silica fume, pre-treated thermally, alkali-activated red mud eventually dissolved to create geopolymer micelles, which coexisted with CSH and densified the microstructure. The pore structure was also improved by the increased alkali concentration [36].

Thus, the use of industrial grade hydrated lime as a solid activator to activate ground granulated blast furnace slag (GGBFS) with silica fume (SF) as an additive appeared exploratory. The same is thus investigated in this brief communication, with the percentages of hydrated lime and SF varying up to 40%.

2. Experimental Methods

The aluminosilicate precursor used in this study was ground granulated blast furnace slag (GGBFS), which was obtained from Rashmi Cement Limited in West Bengal, India. Hydrated lime powder for industry use was purchased locally from Shreeram Chemicals. From Walter Enterprises, silica fume (SF) was purchased. Figure 1 displays the obtained XRD spectra of the precursors and solid activator. Table 1 lists the materials' physical characteristics and chemical make-ups. Modulus of basicity and hydraulic activity are two factors that affect the steel slag's reactivity. The slag must be neutral or basic for alkali activation. The pozzolanic application is better suited for acidic slags. The ratio of total basic oxides to total acidic oxides is known as the modulus of basicity (B) of GGBFS, which equals $(CaO+MgO)/(SiO_2+Al_2O_3)$. Additionally, the GGBFS should meet the BS: 6699 requirements of having a CaO/SiO_2 ratio of less than 1.4. The slag used in this study met the requirements to be used as a precursor for alkali activation with B = 1.14 and CaO/SiO_2 = 1.36.

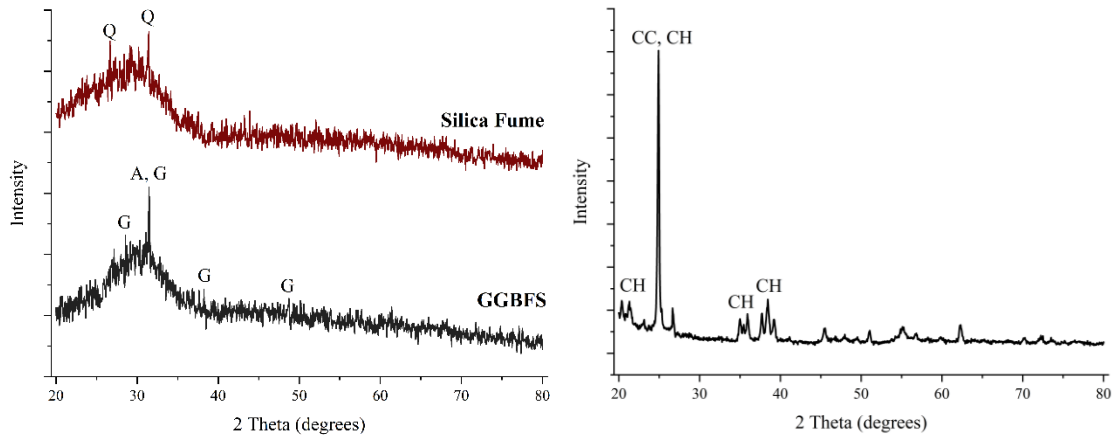

Figure 1: XRD images of the raw materials GGBFS, Silica fume, and Hydrated lime. Q: Quartz, A: Akermenite, G: Gehlenite, CC: Calcium Carbonate, CH: Calcium hydroxide

Table 1: Chemical and physical properties of the raw materials

	Chemical Properties											Physical Properties		
	CaO	SiO_2	Al_2O_3	MgO	MnO	K_2O	Na_2O	Fe_2O_3	TiO_2	P_2O_5	SO_3	Appearance	Density (kg/m^3)	Blaine Fineness (m^2/kg)
GGBS	43.78	32.08	11.20	5.82	0.84	0.42	0.03	0.75	0.87	1.33	1.65	Greyish White	2890	385
SF	3.81	84.12	0.15	1.43	1.15	2.70	0.02	2.64	0.40	0.72	0.33	Greyish Black	2170	589
HL	72.8	1.47	0.87	1.53	0.06	0.04	<0.01	0.36	0.02	-	0.15	Pure White	2240	672

Table 2 shows the different groups of mortar samples formed by varying the silica fume and lime percentages. As a replacement percentage of GGBFS, both lime and silica fume were varied up to 40% addition. Table 2 shows the mix proportions and molar ratios of the samples which are labelled accordingly. The L and SF denote the percentages of lime and silica fume, respectively, with the associated number referring to the percentage. The water/binder ratio in all mixes is 0.45. For the casting of the mortar samples, the aggregate/binder ratio is held constant at 3.0.

To ensure thorough mixing, GGBFS, silica fume, and hydrated lime were dry-mixed in a pan for about a minute. Following that, the standard sand mixture was added to the dry blend, followed by tap water. Each mixing sample was cast in 70.6 mm cubes, in two sets of triplets. They were compacted for 2 minutes in a vibrating machine. The compressive strengths of the mortar samples were assessed after curing for 7 and 28 days, respectively, at room temperature and 100% RH. SEM images were obtained to study the microstructure of the activated mortar samples. Powdered mortar pieces were gathered after samples were tested for compressive strength. The samples were exposed to acetone for 45 minutes, followed by 5 minutes of air drying. After being air dried, the samples underwent a two-hour, 60°C oven drying process. In a vacuum desiccator, the samples are kept until testing for SEM and XRD. The hardened samples with the highest compressive strength are chosen from each group, preferably till 30% of lime addition. Microstructural images were analysed using a FEGSEM (field emission-gun scanning electron microscope), ZEISS Merlin Scanning Electron

Microscope. The acceleration voltage used for all analyses varied between 5-15 kV as per requirement. To ensure precise measurements, the samples were gold-coated prior to testing.

Table 2: Weight fractions of the mix blends using hydrated lime as a solid activator to activate GGBFS with silica fume (SF) as an additive. The variations in the molar ratio are also calculated. The w/b is taken as 0.45 and the aggregate/binder is taken as 3.0.

MIX ID	Wt. fraction of the binder			SiO_2/Al_2O_3	$(CaO + MgO)/SiO_2$	H_2O/CaO
	GGBS	SF	SL			
L10SF10	0.80	0.10	0.10	6.453	0.720	0.033
L10SF20	0.70	0.20	0.10	8.501	0.567	0.036
L10SF30	0.60	0.30	0.10	11.232	0.449	0.040
L10SF40	0.50	0.40	0.10	15.055	0.356	0.046
L20SF10	0.70	0.10	0.20	6.681	0.832	0.031
L20SF20	0.60	0.20	0.20	9.108	0.650	0.034
L20SF30	0.50	0.30	0.20	12.507	0.513	0.037
L20SF40	0.40	0.40	0.20	17.604	0.407	0.042
L30SF10	0.60	0.10	0.30	6.984	0.968	0.029
L30SF20	0.50	0.20	0.30	9.958	0.748	0.032
L30SF30	0.40	0.30	0.30	14.418	0.587	0.035
L30SF40	0.30	0.40	0.30	21.852	0.465	0.038
L40SF10	0.50	0.10	0.40	7.409	1.137	0.027
L40SF20	0.40	0.20	0.40	11.232	0.866	0.030
L40SF30	0.30	0.30	0.40	17.604	0.674	0.032
L40SF40	0.20	0.40	0.40	30.348	0.531	0.036

3. Results and Discussions

The mechanism that occurs when water is added to the mix is $Ca(OH)_2$ hydrolysis into Ca^{-2} and OH^-. The presence of this OH- causes the slag particles to dissociate by breaking the Si-O, Al-O, and Ca-O bonds, resulting in Ca^{+2}, Al^{+3}, $Si(OH)_4$, and $Al(OH)_4^-$. Through polycondensation, $Si(OH)_4$ and $Al(OH)_4^-$ produce dimers of Si-O-Si and Al-O-Al. However, by adding more hydrated lime to the

system, the calcium concentration is increased. Colloidal $Ca(OH)_2$ is also formed as a result of the ongoing process. This combines with the $[SiO_3]^{-2}$ from silica fume to generate C-S-H gels once more. As a result, the two gels coexist and encourage the mix's strength development.

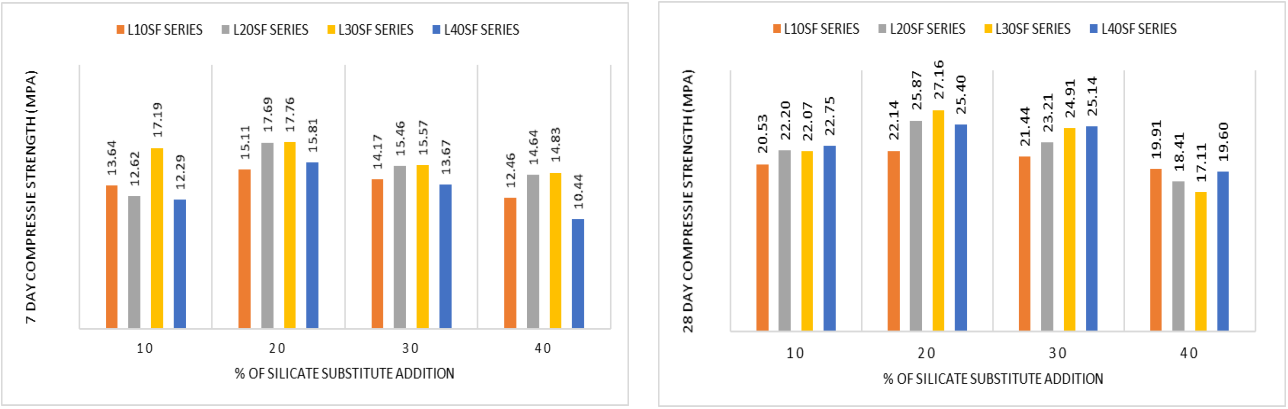

(a) (b)

Figure 2: 7-day and 28-day strength development of the mix blended with SF and activated with hydrated lime (L) with the % variation in the silicate substitute (silica fume) addition

When the proportions of hydrated lime and silica fume were varied in the current investigation, the strength did not change much (see figure 2). Adding more than 30% SF, on the other hand, proved to be unfavourable in every case. Since this did not indicate any systematic variation, strength variation with accordance to the molar ratios were studied. The molar ratios are shown in Table 2 itself. A scattered plot was observed and the best fit of the variation is shown in figure 3 to 5. Both the 7-day and 28-day strength increased as the H_2O/CaO ratio increased. As this would show that GGBFS was dissolved by OH-. However, as GGBFS was not the sole provider of the Ca^{+2} ions, a higher CaO indicated higher possibilities of colloidal $Ca(OH)_2$ formation. Thus, as a secondary reaction product, more CSH would form. As a result, the slope for the 28-day strength development in figure is larger. The SEM pictures also revealed the production of $Ca(OH)_2$ crystals after 7 days of cure. Compressive strength increased when CaO/SiO_2 ratio increased, as shown in the figure. Because Al_2O_3 is a network-constructor in general, increased SiO_2/Al_2O_3 indicated that less Al_2O_3 was available for

polymer network development. This would diminish the possibility of C-A-S-H production and consequently the drop in strength.

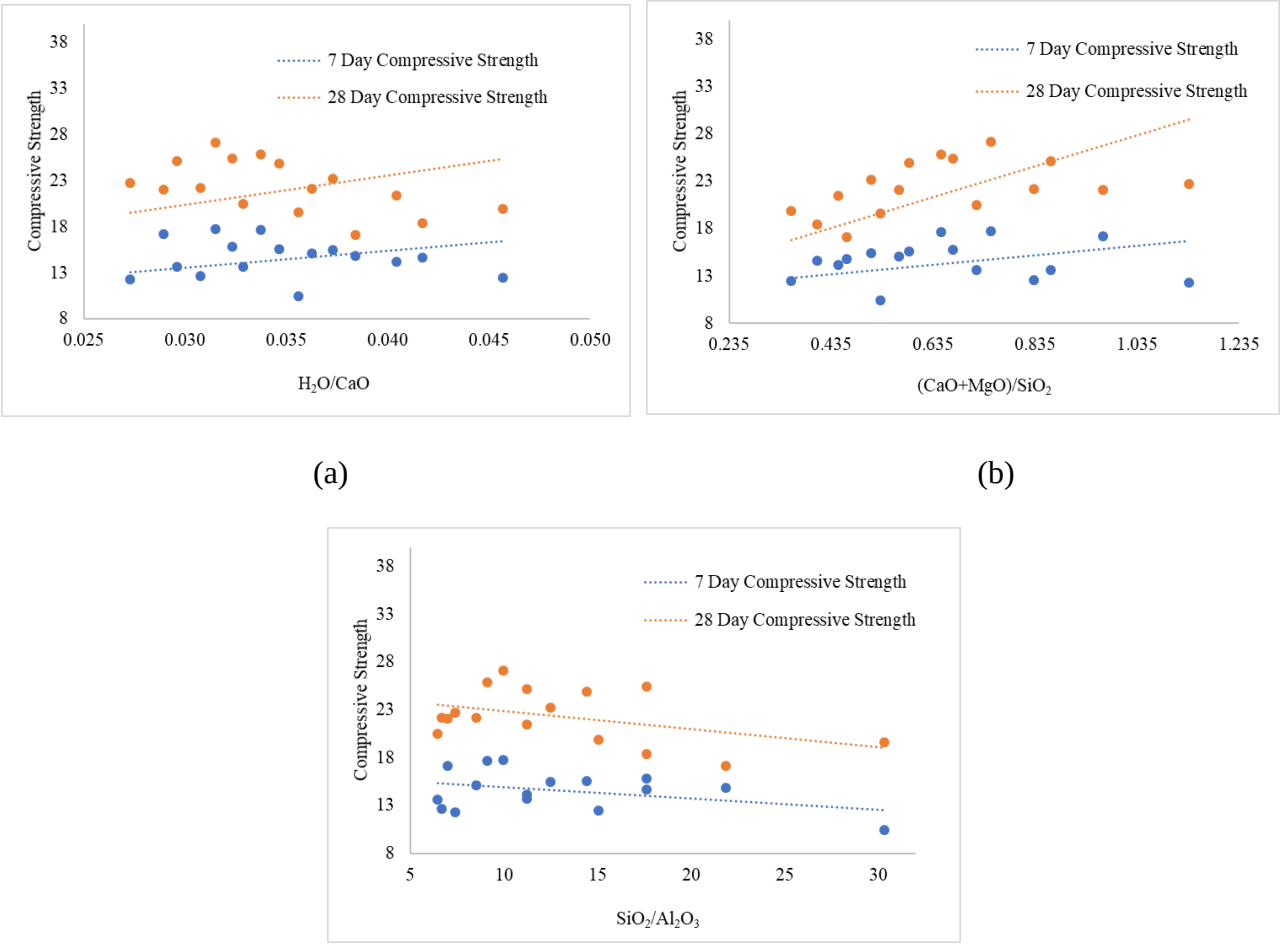

Figure 3: Variation of the compressive strength with the molar ratios

Figure 4 depicts the XRD results of the chosen samples. Calcite (98-011-0799) was the major peak, followed by mineral portlandite (98-005-3829), traces of brucite (98-002-1508), gibbsite (98-012-3163), magnesite (98-002-1915), and quartz (00-033-1161), C-S-H (in the form of Tobermorite 11 A, 98-011-5159), C-A-S-H (in the form of (in the form of Zeolite X, Ca- exchanged, 98-002-8671 and Boggsite, 98-012-2063). Thaumasite, ettringite, and gibbsite correspond to the AFt and AFm phases, indicating that hydration occurred in a manner similar to cement. This crystallinity, as stated in [33], typically weakened the microstructure which also explained the medium strength development in the samples. Again, by regulating the water content the formation of the crystalline

microstructure could be prevented [34]. Figures 5–7 show the corresponding SEM images for L10SF20, L20SF20, and L30SF20. The microstructure was found to be governed more by C-S-H formation than by C-A-S-H formation. Thin hexagonal plate-like formations were also observed in the majority of the 7-day samples, which established the presence of portlandite. The C-S-H fibrous microstructure was visible in the 28-day sample. C-A-S-H was also detected in L20SF20. Fine thaumasite crystals were also visible in L30SF30.

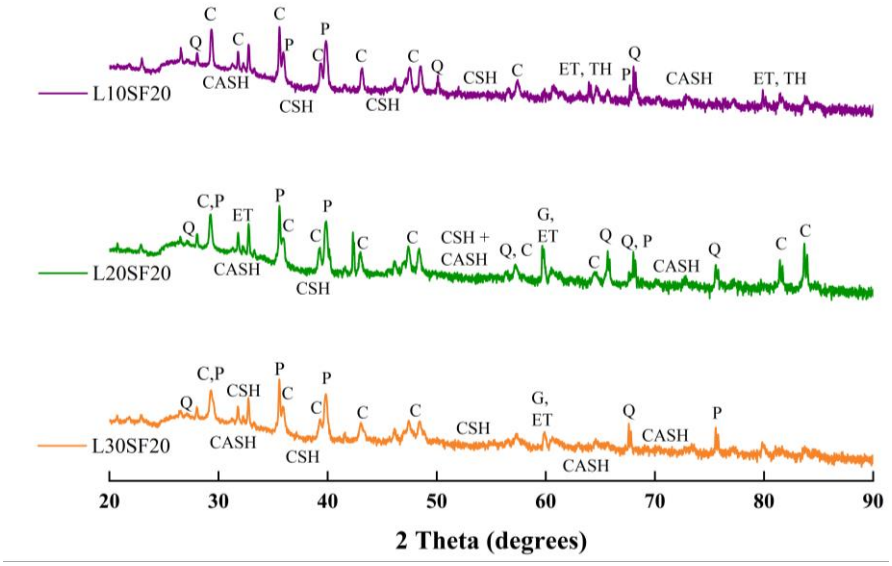

Figure 4: XRD images of L10SF20, L20SF20, and L30SF20 mortar at 28 days. C:Calcite, P: Portlandite, Q: Quartz, G: Gibbsite, ET: Ettringite, TH: Thaumasite

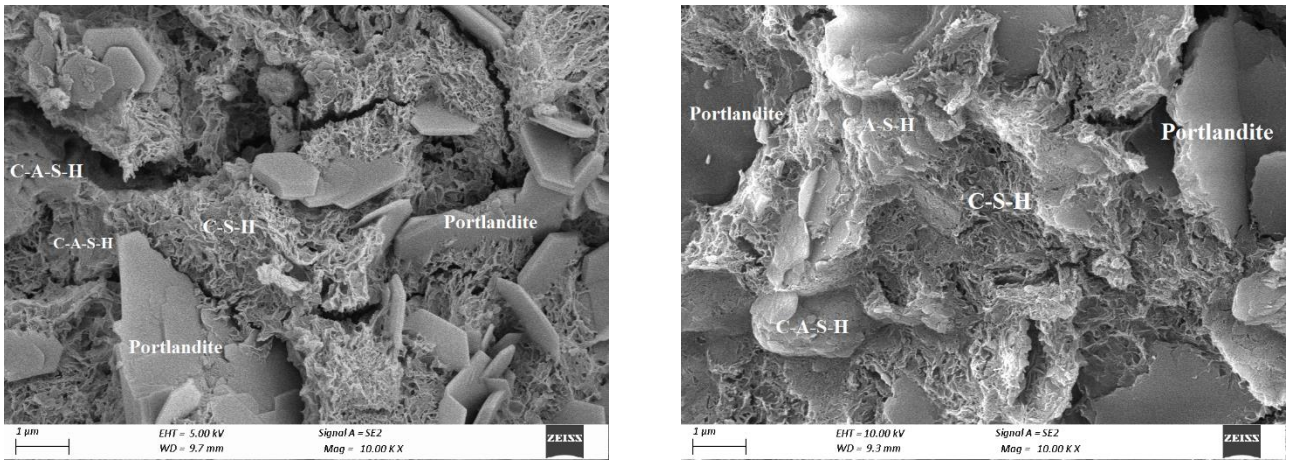

(a) (b)

Figure 5: SEM images of L10SF20 mortar containing 20% hydrated lime and 20% silica fume at (a) 7 days (b) 28 days

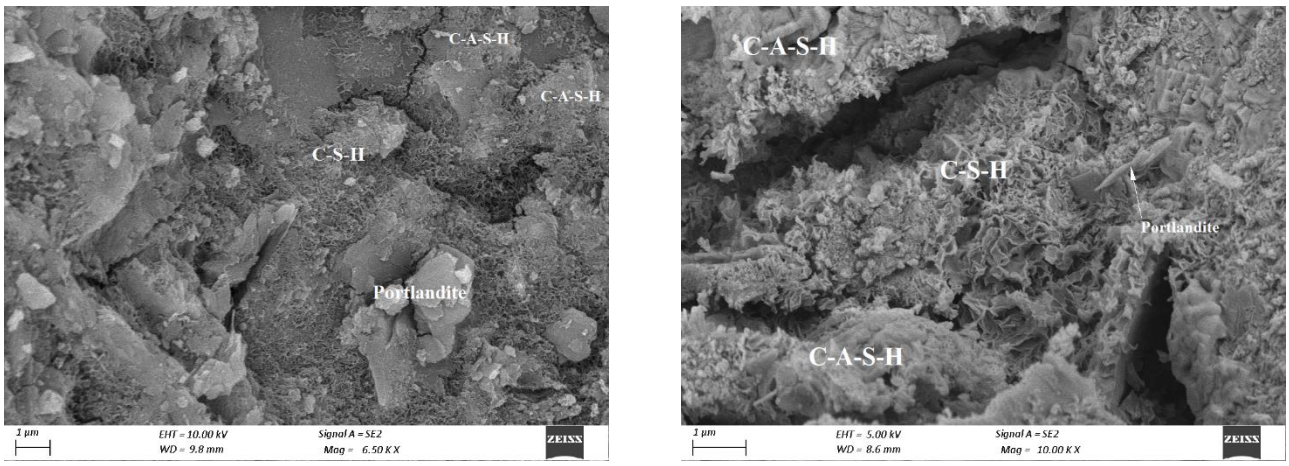

(a) (b)

Figure 6: SEM images of L20SF20 mortar containing 20% hydrated lime and 20% silica fume at (a) 7 days and (b) 28 days.

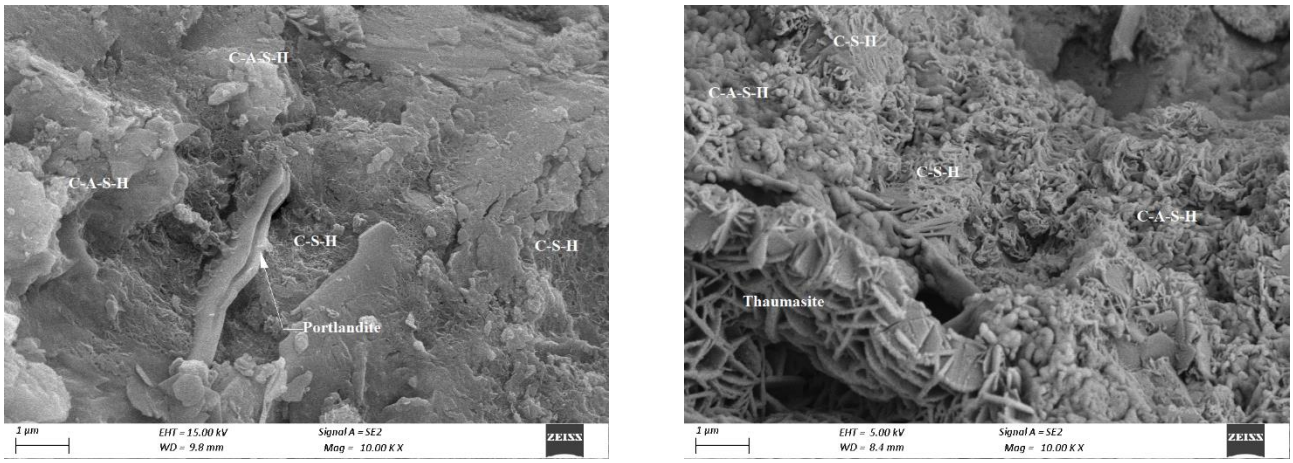

(a) (b)

Figure 7: SEM images of L30SF20 mortar containing 30% hydrated lime and 20% silica fume at (a) 7 days and (c) 28 days.

4. Conclusions

The potential of employing hydrated lime as a solid activator to activate ground granulated blast furnace slag (GGBFS) with silica fume (SF) as an addition was presented in this study, with the percentages of both hydrated lime and silica fume varied up to 40%. The compressive strength did not alter much and varied from 22-25 MPa for 10-30% SF variation; however, at 40% SF replacement,

it reduced to 18-20%. Figure 3 depicts the strength results. The silica fume replacement level can be changed up to 20% for maximum strength, but anything over that was detrimental to strength development. When compared to cement, the 7-day compressive strength reached a high of 17.76 MPa. This was primarily due to an initial lower pH, on addition of water. It is preferable to use a sodium-based activator to keep the system's pH high. C-S-H and C-A-S-H were the primary hydration products. The pozzolanic reaction seemed to have outperformed the polymerization reaction. For the combination of GGBFS and silica fume activated by hydrated lime, the SEM investigation showed that C-S-H governed the microstructural gel. To ensure effective polymerization, the authors intend to perform more research to identify the microstructures in mixes of GGBFS and MS activated by a combination of calcium and sodium-based activators. However, the sodium-based activator should be simple to use and inexpensive.

Acknowledgment

The authors would like to thank the Structural Engineering Laboratory at IIT Kharagpur and the Central Research Facility at IIT Kharagpur for their assistance with the experiments.

References

[1] S. Louati, S. Baklouti and B. Samet, "Geopolymers Based on Phosphoric Acid and Illito-Kaolinitic Clay," *Advances in Materials Science and Engineering,* pp. 1-7, 2016.

[2] S. Louati, S. Baklouti and B. Samet, "Acid based geopolymerization kinetics: Effect of clay particle size," *Applied Clay Science,* vol. 132–133, p. 571–578, 2016.

[3] Y. He, L. Liu, L. He and X. Cui, "Characterization of chemosynthetic H3PO4–Al2O3–2SiO2 geopolymers," *Ceramics International* , vol. 42, p. 10908–10912, 2016.

[4] L. Le-ping, C. Xue-min, H. Yan, L. Si-dong and G. Si-yu, "The phase evolution of phosphoric acid-based geopolymers at elevated temperatures," *Materials Letters,* vol. 66, p. 10–12, 2012.

[5] H. Celerier, J. Jouin, V. Mathivet, N. Tessier-Doyen and S. Rossignol, "Preparation and characterization of acid-based geopolymer using," *Journal of Non-Crystalline Solids* , vol. 493, p. 94–98, 2018.

[6] Y.-S. Wang, J.-G. Dai, Z. Ding and W.-T. Xu, "Phosphate-based geopolymer: Formation mechanism and thermal stability," *Materials Letters* , vol. 190, p. 209–212, 2017.

[7] L. Xu, F. Matalkah, P. Soroushian, N. Darsanasiri, S. Hamadneh and W. Wu, "Effects of citric acid on the rheology, hydration and strength development of alkali aluminosilicate cement," *Advances in Cement Research,* pp. 1-8, 2017.

[8] R. Vallepu, A. Fernández-Jiménez, T. Terai, A. Mikuni, A. Palomo, K. MacKenzie and K. Ikeda, "Effect of synthesis pH on the preparation and properties of K–Al-bearing silicate gels from solution," *Journal of Ceramic Society,* vol. 114, p. 624–629, 2006.

[9] F. Matalkah, L. Xu, W. Wu and P. Soroushian, "Mechanochemical synthesis of one-part alkali aluminosilicate hydraulic cement," *Materials and Structures,* vol. 50, p. 97, 2017.

[10] I. Garcia-Lodeiro, A. Palomo, A. Fernández-Jiménez and D. Macphee, "Compatibility studies between N-A-S-H and C-A-S-H gels. Study in the ternary diagram Na2O–CaO–Al2O3–SiO2–H2O," *Cement and Concrete Research,* vol. 41, p. 923–931, 2011.

[11] C. Yip, G. Lukey and J. v. Deventer, "The coexistence of geopolymeric gel and calcium silicate hydrateat the early stage of alkaline activation," *Cement and Concrete Research,* vol. 35, pp. 1688-1697, 2005.

[12] W. K. W. Lee and J. S. J. v. Deventer, "The effect of ionic contaminants on the early-age properties of alkali-activated fly ash-based cements," *Cement and Concrete Research* , vol. 32, pp. 577-584, 2002.

[13] P. Chindaprasirt, C. Jaturapitakkul, W. Chalee and U. Rattanasak, "Comparative study on the characteristics of fly ash and bottom ash geopolymers," *Waste Management,* vol. 29, p. 539–543, 2009.

[14] J. Peyne, J. Gautron, J. Doudeau, E. Joussein and S. Rossignol, "Influence of calcium addition on calcined brick clay based geopolymers: A thermal and FTIR spectroscopy study," *Construction and Building Materials* , vol. 152, pp. 794-803, 2017.

[15] D. Jeon, Y. Jun, Y. Jeong and J. E. Oh, "Microstructural and strength improvements through the use of Na2CO3 in a cementless Ca(OH)2-activated Class F fly ash system," *Cement and Concrete Research,* vol. 67, pp. 215-225, 2015.

[16] F. Massazza, "Pozzolanic cements," *Cement and Concrete Composites,* vol. 15, no. 4, 1993.

[17] E. Vejmelková, M. Keppert, P. Rovnaníková, Z. Keršner and R. Černý, "Properties of lime composites containing a new type of pozzolana for the improvement of strength and durability," *Composites Part B: Engineering,* vol. 43, no. 8, 2012.

[18] M. D. Jackson, S. R. Chae, S. R. Mulcahy, C. Meral, R. Taylor, P. Li, A.-. Emwas, J. Moon, S. Yoon, G. Vola, H.-. Wenk and P. J. Monteiro, "Unlocking the secrets of Al-tobermorite in Roman seawater concrete," *American Mineralogist,* vol. 98, pp. 1669-1687, 2013.

[19] M. D. Jackson, S. R. Mulcahy, H. Chen, Y. Li, Q. Li, P. Cappelletti and H.-R. Wenk, "Phillipsite and Al-tobermorite mineral cements produced through low-temperature water-rock reactions in Roman marine concrete," *American Mineralogist,* vol. 102, p. 1435–1450, 2017.

[20] J. Davidovits, "Geopolymers: Inorganic Polymeric New Materials," *Journal of Thermal Analysis,* vol. 37, pp. 1633-1656, 1991.

[21] V. Pavlík and M. Uzˇáková, "Effect of curing conditions on the properties of lime, lime–metakaolin and lime–zeolite mortars," *Construction and Building Materials,* vol. 102, pp. 14-25, 2016.

[22] M. Stefanidou, E.-. C. Tsardaka and E. Pavlidoub, "Influence of nano-silica and nano-alumina in lime-pozzolan and lime-metakaolin binders in 13th International Conference on Nanosciences & Nanotechnologies," *Materials Today: Proceedings,* vol. 4, p. 6908–6922, 2017.

[23] H. M, E. H, E.-D. H, H. M, K. K and E.-S. A, "Pozzolanic activity of silica fume with lime," *Journal of Basic and Environmental Sciences,* vol. 4, pp. 236-246, 2017.

[24] J. M. Paris, J. G. Roessler, C. C. Ferraro and H. D. DeFord, "A review of waste products utilized as supplements to Portland cement in concrete," *Journal of Cleaner Production* , vol. 121, pp. 1-18, 2016.

[25] C. Shi, A. F. Jiménez and A. Palomo, "New cements for the 21st century: The pursuit of an alternative to Portland cement," *Cement and Concrete Research,* vol. 41, pp. 750-763, 2011.

[26] Juenger, M. C.G. and Rafat, "Recent advances in understanding the role of supplementary cementitious materials in concrete," *Cement and Concrete Research,* vol. 78, p. 71–80, 2015.

[27] E. Aprianti, P. Shafigh, S. Bahri and J. N. Farahani, "Supplementary cementitious materials origin from agricultural wastes – A review," *Construction and Building Materials,* vol. 74, p. 176–187, 2015.

[28] M. Frías, O. Rodríguez and M. S. de Rojas, "Paper sludge, an environmentally sound alternative source of MK-based cementitious materials. A review," *Construction and Building Materials,* vol. 74, p. 37–48, 2015.

[29] K. H. Mo, U. J. Alengaram, M. Z. Jumaat, S. P. Yap and S. C. Lee, "Green concrete partially comprised of farming waste residues: a review," *Journal of Cleaner Production,* vol. 117, pp. 122-138, 2016.

[30] J. L. Provis, A. Palomo and C. Shi, "Advances in understanding alkali-activated materials," *Cement and Concrete Research,* vol. 78, p. 110–125, 2015.

[31] T. Luukkonen, Z. Abdollahnejad, J. Yliniemi, P. Kinnunen and M. Illikainen, "One-part alkali activated materials: A review," *Cement and Concrete Research,* vol. 103, pp. 21-34, 2018.

[32] N. Ye, J. Yang, S. Liang, Y. Hu, J. Hu, B. Xiao and Q. Huang, "Synthesis and strength optimization of one-part geopolymer based on red mud," *Construction and Building Materials* , vol. 111, pp. 317-325, 2016.

[33] B. Zhang, K. J. D. MacKenzie and I. W. M. Brown, "Crystalline phase formation in metakaolinite geopolymers activated with NaOH and sodium silicate," *Journal of Materials Science,* vol. 44, no. 17, p. 4668–4676, 2009.

[34] A. Hajimohammadi and J. S. J. v. Deventer, "Solid Reactant-Based Geopolymers from Rice Hull Ash and Sodium Aluminate," *Waste Biomass Valor,* vol. 8, pp. 2131-2140, 2017.

[35] Y. J. Patel and N. Shah, "Enhancement of the properties of Ground Granulated Blast Furnace Slag based Self Compacting Geopolymer Concrete by incorporating Rice Husk Ash," *Construction and Building Materials,* vol. 171, pp. 654-662, 2018.

[36] Y. Y. Kim, B.-J. Lee, V. Saraswathy and Seung-Jun-Kwon, "Strength and Durability Performance of Alkali-Activated Rice HUsk Ash Geopolymer Mortar," *The Scientific World Journal* , vol. 2014, pp. 1-10, 2014.